TRANSIENT NATURAL CONVECTION FLOW ON AN ISOTHERMAL VERTICAL WALL AT HIGH PRANDTLNUMBERS: SECOND-ORDER APPROXIMATION

A. Baradaran Rahimi and E. Yousefi

Faculty of Engineering, Ferdowsi Univ. of Mashhad
Mashhad, Iran, rahimiab@yahoo.com

(Received: May 5, 2000 - Accepted in Revised Form: July 18, 2001)

Abstract The method of matched asymptotic expansions, which has been used in previous studies of steady natural convection flow, is extended here to transient natural convection flow at high Prandtl number (Pr). Second-order expansion solutions, valid for large Prandtl numbers, are presented for the transient natural convection flow near a vertical surface which undergoes a step change in temperature. Throughout the transient, the flow is found to have the same dual-layer structure which is characteristic of the steady flow at high Prandtl number. For large Prandtl number, the time to steady state is shown to increase proportional to square root of Pr. The temperature and velocity overshoot, which occurs during the transient at moderate Prandtl number, is shown to disappear as Pr $\to \infty$. Uniformly valid expansions for the velocity and temperature profiles near the surface are found to be in good agreement with the numerical solution of the full governing equations for as low as Pr=16. By increase of Prandtl number, the error because of instability in numerical solution of the full governing equations increases and the necessity of using singular perturbation techniques become more obvious.

Key Words Transient, Natural Convection, Isothermal Wall, High Prandtl, Perturbation

oŠ¯ nj nAk½BQ S$Be ºlo‖ ° jApC»½B\‖B] ¬B½o] nj »¦L› RBíS$B†« nj ³Ÿ »L¯B\« ˜BL†¯A ...v‖ x °n **²k¼ña** ¨°j ³LJo« ¥e/j±{»« ²jAj ©½ª íU ònq‖¥T¯AoQ jkî B‖Anm£ S$Be nj jApC»½B\‖B] ºlo‖B\@½A nj,SwA ²k{ ³T–o£¦ ºj±ªî ¶nA±½j ð½ »ñ½jq¯ njAnm£ S$Be jApC»½B\‖B] ¬B½o] ºlo‖,SwA oLTí« ònq‖¥T¯AoQB‖ jAkîA ºlo‖ ³Ÿ ...v‖ »½BU°j nBT i Bw¬B½o] ,Anm£ S$Be owBlow nj /©¼µj»« ³ÅnABl\@½A nj An j±{»« é›A° B«j ºA³¦Q RAo½¼'U Sdl ³Ÿ¦ nAk½BQ S$Be ³‖ ¬B«p ,ònq‖¥T¯AoQ jAkîA ºlo‖/k{B‖»« ¿B‖ ¥T¯AoQ jAkîA ºlo‖ ° nAk½BQ S$Be nj ¬B½o] ³‖Bz« ³Ÿ jnAj Sªw ³‖¥T¯AoQ jkî »T›° Sîow° B«j ºBµnAj±ª¯nj j±]±« ºBµB† i /k‖B½»« y ¼q–A¥T¯AoQ jkî nm] B‖ KwB®T« »‖± i SšlB†« ²nA±½j »ñ½jq¯ nj Rnbe³]nj ° Sîow ºlo‖ oLTí« ºB´†v‖/k¯°n»« -¼‖ pA,k@Ÿ»« ¥¼« S½B´®‖ ©ŸBe R¿jBí« ºjkî ¥e nj B† i ,¥T¯AoQ jkî y ¼q–AB‖/k¯nAj²jq¯B{¥T¯AoQ jkî BU ©ŸBe R¿jBí« ºjkî ¥e B‖ /j±{»« pod«oTz¼‖ jo–®« -z¼‖n±‖oQ x °n pA²jB–TwA ³‖ ZB¼TeA° ³T–B½ y ¼q–A

INTRODUCTION

The transient laminar fluid motion and heat transfer resulting from the impulsive heating or cooling of a vertical surface in a quiescent fluid has been the subject of a number of previous studies. For both the step change in temperature for the iso-thermal surface, and the sudden application of a uniform heat flux, analytical solutions have been obtained [1,2] for the one dimensional portion of the transient. Finite-difference computational schemes [3,4] have been used to predict the transport behavior during the entire transient, including both the one-dimensional regime and the later period, during which the flow adjusts to its steady-state two-dimensional form.

Although these studies have thoroughly investigated the important flow and heat transfer phenomena in transient natural convection near vertical surfaces, they provide very little information about the systematic behavior of such flows at high Prandtl number. The finite difference calculations which have been made for these flows, have been at Prandtl numbers near 1, for gases, or near 7, for water.

The closed-form solutions for the one-dimensional portion of the transient may be evaluated for any Prandtl number, but they are valid only for short times. Gebhart [5] presented solutions for the uniform-flux surface for values of Prandtl number up to 1000. However, the accuracy of these solutions is limited by the assumption of the integral method. Almost all experimental data on transient vertical natural convection flows have also been from flows in fluids with Prandtl numbers near either 1 or 7.

The limiting case solutions [Ref. 2] when Prandtl number is taken as infinity, omits the derivative term of second-order in energy equation and change it into a partial differential equation of first-order. This reduction is only valid in limiting studies when Prandtl number is exactly infinity. But physically in some applications fluids are employed which have the property of having high Prandtl number other than exactly infinity.

The present work is an analysis of transient natural convection in a high Prandtl number fluid. The analysis is applied to an isothermal surface which suddenly changes temperature above or below the ambient. Flows of this type commonly occur in technological applications. A high Prandtl number fluid is sometimes used as a heat sink in electrical transformers. The sudden application of electrical power to the transformer produces a transient buoyancy-driven flow. Transient flows at high Prandtl number may also result from the sudden addition or removal of heat in chemical processing of hydrocarbon and silicone polymers, and in thermal energy storage devices.

The analysis used here combines a matched asymptotic expansion technique [6] with an explicit finite difference computational scheme. Asymptotic transient profiles are obtained for the limiting circumstances of Pr $\to\infty$. Second-order corrections are also computed so the results may be used to predict flow and heat transfer at moderate values of Pr. It will be shown that the results accurately predict the flow and temperature field behavior at least in the range 16<Pr< ∞. These results provide a more complete picture of the manner in which the heat transfer and flow behavior changes with Prandtl number in these time-dependent flows.

FORMULATIONOF THE PROBLEM

The analysis applies to a flat vertical plate immersed in an extensive body of quiescent fluid at a uniform temperature. To initiate the transient, the plate temperature is suddenly raised or lowered to a value different from the temperature of the fluid.

The analysis incorporates the non-dimensional variables of Hellums and Churchill [7], listed below

$$T_N - \frac{T - T_\infty}{T_w - T_\infty} - \frac{T - T_\infty}{\Delta T}$$

$$U - u\,(\nu g\beta, \Delta T)^{-1/3}$$

$$V = \nu\,(\nu g\beta_t \Delta T)^{-1/3}$$

$$Y = y\left(g\beta_t \frac{\Delta T}{\nu^2}\right)^{1/3} = \frac{y}{x} Gr_x^{1/3} \qquad (1)$$

The equations governing conservation of mass, momentum and energy, in terms of these non-dimensional variables, are given below. The usual boundary-layer and Boussinesq approximations have been made:

$$\frac{\partial U}{\partial X} + \frac{\partial V}{\partial Y} = 0$$

$$\frac{\partial U}{\partial \tau} + U\frac{\partial U}{\partial X} + V\frac{\partial U}{\partial Y} = T_N + \frac{\partial^2 U}{\partial Y^2}$$

$$\frac{\partial T_N}{\partial \tau} + U\frac{\partial T_N}{\partial X} + V\frac{\partial T_N}{\partial Y} = \frac{1}{Pr}\cdot\frac{\partial^2 T_N}{\partial Y^2} \qquad (2)$$

The initial and boundary conditions are

$$\tau = 0 : U = V = T_N = 0 \qquad (3a)$$

$$X = 0 : U = V = T_N = 0 \qquad (3b)$$

$$Y = 0 : U = V = 0 , T_N = 1 \qquad (3c)$$

$$Y \to \infty : U = T_N = 0 \qquad (3d)$$

As $Pr \to \infty$, the coefficient of the second derivative in the energy equation vanishes. Hence, to obtain a solution for large Pr, a singular perturbation technique is needed. It is therefore assumed that throughout the transient, the flow consists of two regions: an inner region, near the surface, dominated by buoyancy and viscous effects, and an outer region where only viscous and momentum effects are important. Accordingly, in the inner region, the Y and time coordinates are stretched as follows

$$\varepsilon \quad \frac{1}{Pr} \;, \; Pr \to \infty \tag{4}$$

$$\eta \quad \varepsilon^{-1/4} \, Y \qquad , \theta \quad \varepsilon^{1/2} \, \tau \tag{5}$$

Inner expansions for U, V and T are taken to be

$$U_i = \varepsilon^{1/2} \left[U_0 + \varepsilon^{1/2} U_1 + \varepsilon U_2 \quad \ldots \right]$$

$$V_i - \varepsilon^{3/4} \left[V_0 + \varepsilon^{1/2} V_1 + \varepsilon V_1 - \ldots \right]$$

$$T_i - T_N - \left[T_0 - \varepsilon^{1/2} T_1 - \varepsilon T_2 - \ldots \right] \tag{6}$$

The inner variables and expansions are chosen so that, to lowest order, as $Pr \to \infty$, the inner momentum equation retains only the viscous and buoyancy terms.

Writing the governing equations (2) in terms of the inner coordinates (5) and expansions (6), and requiring that the equations be satisfied at each level in powers of ε, the systems of equations for inner region are obtained which are presented in Appendix as Equations I, II, and III.

In similar fashion, outer stretched coordinates and expansions are taken to be

$$\xi - \varepsilon^{1/4} Y \quad , \quad \theta - \varepsilon^{1/2} \tau \tag{7}$$

$$U^0 - \varepsilon^{1/2} \left[u_0 - \varepsilon^{1/2} u_1 + \varepsilon \; u_2 + \ldots \right]$$

$$V^0 - \varepsilon^{1/4} \left[v_0 - \varepsilon^{1/2} v_1 + \varepsilon \, v_2 + \ldots \right]$$

$$T^0 = 0 \tag{8}$$

The scaling and expansions are chosen so that, to lowest order, only momentum and viscous terms are retained. The temperature field is exponentially small in the outer region and is therefore taken as zero in the expansion to $O(\varepsilon)$.

Substituting in the same manner as for the inner equations, the systems of equations are obtained for the outer velocity terms which are presented in Appendix as Equations IV, V, and VI.

Boundary conditions at the surface (η=0) and initial conditions for the inner equations are obtained by substituting new variables (5) and the expansions (6) into Equations 3a-3c. Likewise, the boundary conditions far from the surface and the initial conditions for the outer equations are obtained by substituting the relations in (7) and (8) into Equations 3a, 3b and 3d.

The outer ($\eta \to \infty$) boundary conditions for the inner equations and the inner ($\xi \to 0$) boundary conditions for the outer equations are obtained by matching the inner and outer expansions. The method used here is similar to that described by Van Dyke [8] except that the x and time dependence of the flow field must be considered. Since the inner and outer x(X) and time (θ) scales are equal, the inner and outer expansions can be matched for fixed X and θ. Combining the matching conditions with the required conditions at $\theta = 0$, $X = 0$, $\eta = 0$ and $\xi = \infty$, the full boundary and initial conditions for the inner and outer equations are obtained.

CALCULATION PROCEDURE

The systems of Equations I, II, III and IV, V, VI together with the corresponding boundary and initial conditions were solved numerically using an explicit finite difference scheme. The value $X_{max} - 100$ was considered to represent the total height of the plate, and $\eta_{max} - \xi_{max} - 16$ were considered to represent $\eta - \infty$ and $\xi = \infty$. This is equivalent to a value of the Grashof number, Gr_x, of 10^6 at the end of the plate.

The flow region was divided into a grid with m and n spacings in the X and Y directions. For

both the inner and outer regions, the values of m and n used were 20 and 32, respectively. Second-order derivatives were written in central differences, forward differences were used for first-order derivatives in η, ξ and θ, and a backward difference was used for X derivatives.

The calculation procedure generates a solution by marching forward in time while matching the inner and outer expansions at each time step. Beginning with the results from the last time step, the solution at the next step was calculated first for the lowest-order inner equations along with their corresponding conditions using the newly calculated necessary values, the lowest-order outer solution was then calculated for next time step. This procedure were followed to solve the higher order inner and outer equations. The resulting velocity and temperature fields were then stored, and the whole process was repeated to march the entire perturbation solution forward in time. The solution was computed until steady state was reached using a time step, $\Delta\theta$, of 0.01.

From a series of calculations with different grid sizes and time steps, it was calculated that m=20, n=32 and $\Delta\theta$ = 0.01 would yield acceptable accuracy. Increasing $\Delta\theta$ from 0.01 to 0.02 resulted in a change in the velocity and temperature profiles of less than 2% of their respective peak values across the layer.

It should be mentioned here that in order to control our computer code and for the purpose of comparison, the full governing equations (2) along with initial and boundary conditions (3) were also solved numerically with similar procedures as above.

RESULTS AND DISCUSSIONS

In addition to the numerical solution of the full governing equations, the following one-dimensional analysis can also be used for the sake of comparison with the perturbation solutions.

During the initial one-dimensional portion of the transient, the V-velocity and X-derivative terms in the governing equations are zero. Without these terms, the governing equations and boundary conditions reduce to a linear system of partial differential equations and boundary conditions for which closed-form solutions exist. Using Laplace Transformations, it is easily shown that during the one-dimensional portion of the transient, the solutions for governing equations of the inner and outer regions with corresponding boundary conditions are given by

$$T_0 = erfc\left[\frac{\eta}{2\sqrt{\theta}}\right], \quad T_1 = T_2 = 0 \tag{9}$$

$$U_0 = \theta \cdot \left[\left(\frac{\eta}{\sqrt{\theta}}\right) - \frac{\eta}{\sqrt{\pi\theta}} \cdot exp\left(\frac{\eta^2}{4\theta}\right) \right] \tag{10}$$

$$U_1 = -2\eta \cdot \sqrt{\frac{\theta}{\pi}}, \quad U_2 = 0 \tag{11}$$

$$u_0 = \left[\left(\xi^2 \right) \right] \cdot \left[\xi \right] - \frac{\xi}{\sqrt{\pi\theta}} \cdot exp\left(-\frac{\xi^2}{4\theta}\right), \quad u_1 = u_2 = 0 \tag{12}$$

The solution for the lowest-order temperature solution is just the one-dimensional conduction transient in a semi-infinite solid. The lowest-order inner and outer solutions for the velocity, obtained above, can be combined using the method of additive composition, described by Van Dyke [8], to obtain the following uniformly valid solution for the U velocity:

$$U_c(\tau, Y) = \tau\varepsilon \left[\left(1 + \frac{Y^2}{2\tau}\right) \cdot erfc\left(\frac{Y}{2\sqrt{\tau}}\right) - \frac{Y}{\sqrt{\pi\tau}} \cdot exp\left(\frac{-Y^2}{4\tau}\right) - \left(1 - \frac{Y^2}{2\tau\varepsilon}\right) \right] \left[erfc\left[\frac{Y}{2\sqrt{\tau\varepsilon}}\right] + \frac{Y}{\sqrt{\pi\tau\varepsilon}} exp\left(-\frac{Y^2}{4\tau\varepsilon}\right) \right] + \ldots \tag{13}$$

The uniformly-valid solution for U, Equation 22, is compared with the corresponding one-dimensional solution obtained from governing Equations 2, as following:

$$\frac{U_c(\tau, Y, \varepsilon)}{U(\tau, Y, \varepsilon)} = (1 \quad \varepsilon) \tag{14}$$

It is seen from (14) that as Pr $\rightarrow \infty$, these two solutions are the same. On the other hand, from the one-dimensional governing Equations 2 and their corresponding initial and boundary conditions, we get

$$\Rightarrow \quad T_N(Y, \tau) - erfc\left[\frac{Y}{2\sqrt{\varepsilon\tau}}\right] \tag{15}$$

Also from $q'' = K\frac{\partial T}{\partial y}\Big|_{y \quad 0} = h\Delta T$, the local Nusselt Number from (9) and (15) is

$$Nu_x - \frac{Gr_x^{/3} \cdot \varepsilon^{1/4}}{\sqrt{\pi\theta}} \quad , \qquad Nu_x - \frac{Gr_x^{/3}}{\sqrt{\pi\varepsilon\tau}} \tag{16}$$

To obtain the second-order approximate solution of two-dimensional composite solution which is uniformly valid every where, an asymptotic matching procedure as before is used, to get

$$U_c - \varepsilon^{1/2} \; \bar{U}_0 + u_0 - A_{00} + \varepsilon^{/3} \left(U_1 + u_1 + \right.$$

$$A_{10} \quad A_{11} \cdot \eta \qquad \varepsilon \quad U_2 \quad u_2$$

$$\left. A_{20} - A_{21} \cdot \eta - A_{22} \cdot \frac{\eta^2}{2} \right) \Big] \tag{17}$$

where the functions A00, A10, A11, A20, A21, and A22 are presented in the Appendix as equations (VII).

From the expansion for the temperature field, the local Nusselt number is related to the gradients of T0, T1, and T2 at the surface as

$$Nu_x \quad -\varepsilon^{1/4} \cdot Gr_x^{1/3} \left[\frac{\partial T_0}{\partial \eta}(X, 0, \theta) + \varepsilon^{1/2} \right.$$

$$\left. \frac{\partial T_1}{\partial \eta}(X, 0, \theta) + \varepsilon \frac{\partial T_2}{\partial \eta}(X, 0, \theta) \right] \tag{18}$$

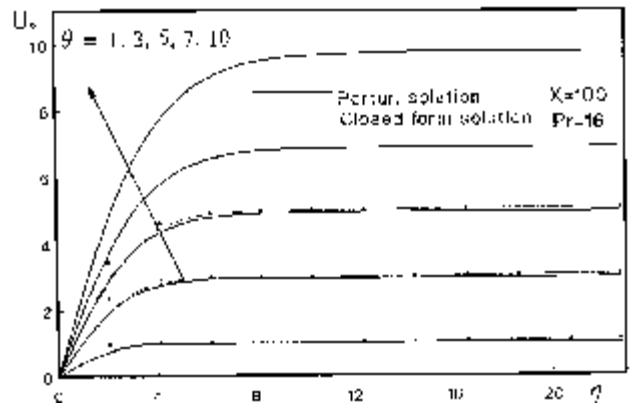

Figure 1. Lowest-order inner velocity profile for Pr = 16, for two-dimensional (---) and one-dimensional case (- - -).

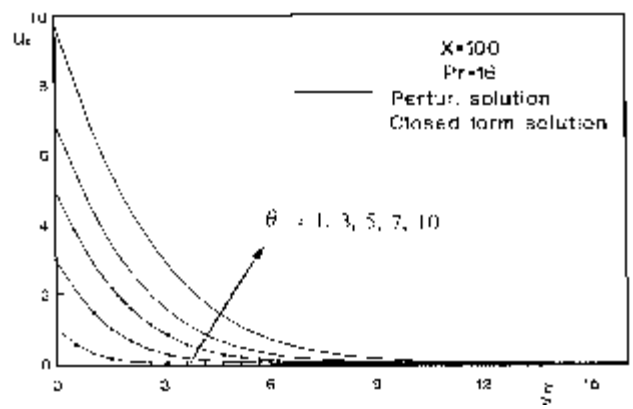

Figure 2. Lowest order outer velocity profile for Pr = 16, for two-dimensional (---) and one-dimensional case (- - -).

It can easily be shown that during the initial one-dimensional portion of the transient, and at steady state, the heat transfer parameter $Nu_x / Gr_x^{/4}$ is a function only of the ratio $\tau / X^{1/2}$.

Figure 1 shows the lowest-order inner velocity profile for Pr= 16 at the end of the plate (X= 100) for two-dimensional (---) and one-dimensional (- - -) case for various values of θ. These results compare very well for small θ and indicates the accuracy of our computer code. Figure 2 shows the lowest-order outer velocity profile in the case of two-dimensional (---) and one-dimensional (- - -) for Pr=16 and

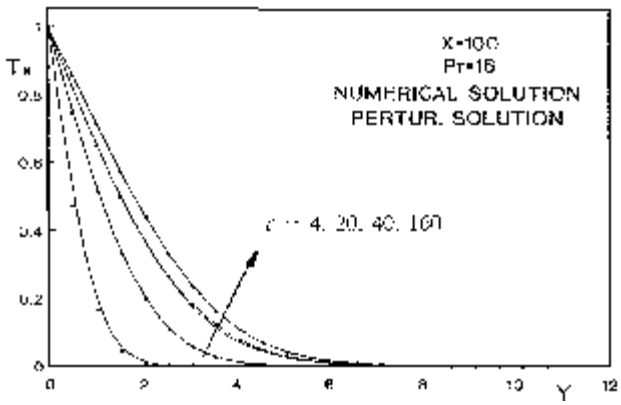

Figure 3. Variation of temperature for Pr = 16 for different values of t. Complete numerical solution (---) and perturbation solution (- - -).

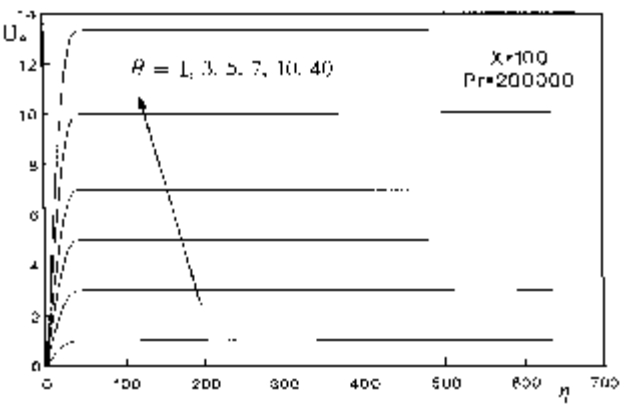

Figure 4. Lowest-order inner velocity profile for different values of q for Pr = 2000.

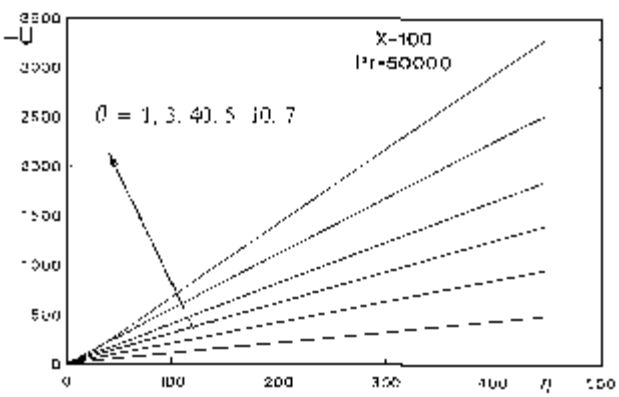

Figure 5. First-order inner velocity profile for different values of q for Pr = 20,000.

for different values of q. Figure 3 shows the variations of temperature for Pr=16 at the end

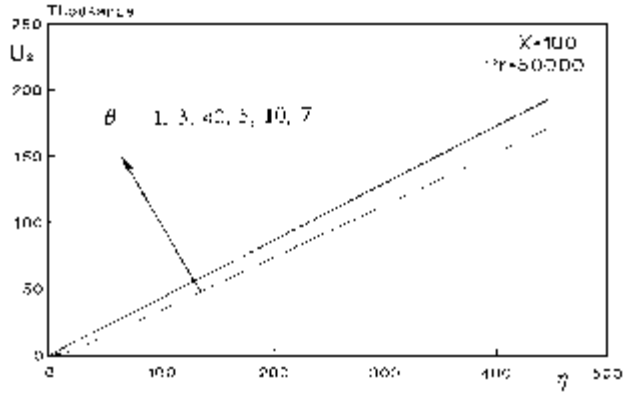

Figure 6. Second-order inner velocity profile for different values of q for Pr = 50,000.

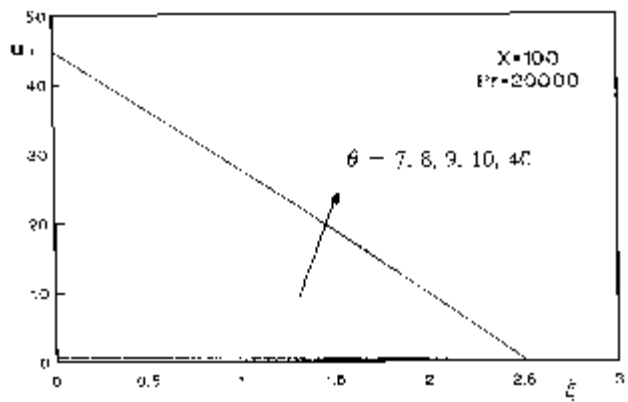

Figure 7. First-order outer velocity profile for different values of q for Pr = 20,000.

of the plate (X= 100) for the case of complete numerical solution of the equations (---) and perturbation solution (- - -) for different values of t. Figure 4 shows the variation of lowest-order inner velocity for Pr=20000 at the end of plate (X=100) for different values of q. As it can be seen, by increasing Pr the curves quickly reach a maximum and then reach a constant value. Figure 5 shows the variations of first-order inner velocity at Pr= 50000 for different values of q. As it is seen these curves do not intersect but because of effects of momentum in the inner region and for low values of Pr these curves have intersections. Figure 6 shows the variations of second-order inner velocity at Pr= 50000 for different values of q. Figure 7 shows the variations of first-order outer velocity at Pr= 20000 for different values of q. Figure 8 shows the variations of

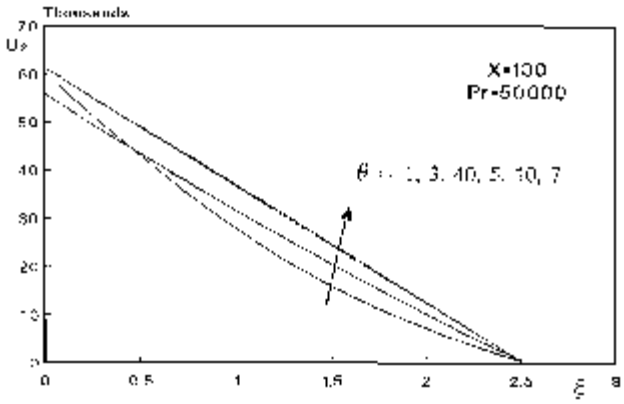

Figure 8. Second-order outer velocity for different values of q for Pr = 50,000.

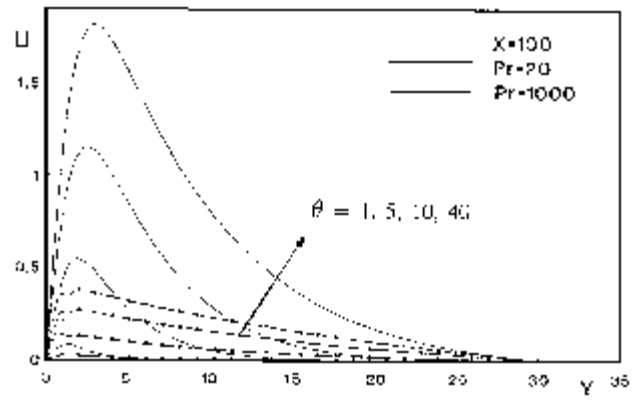

Figure 10. Velocity profile for different values of q for Pr = 20 (---), Pr = 1000 (- - -).

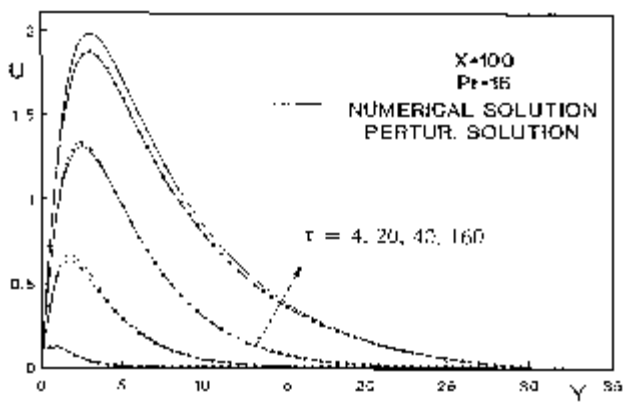

Figure 9. Velocity profile for different values of t for Pr = 16. Complete numerical solution (---) and perturbation solution (- - -).

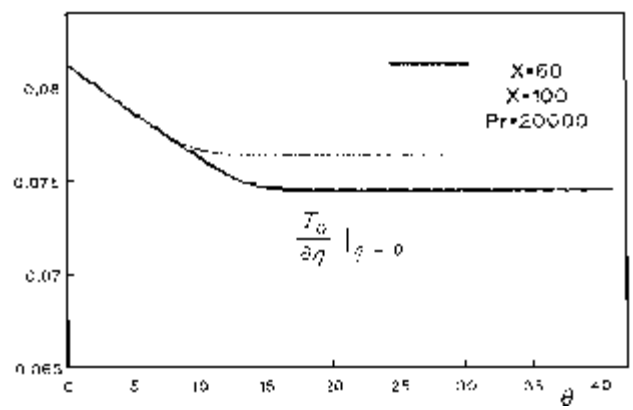

Figure 11. Gradient of T0 on the wall at X = 100(---) and X = 60 (- - -), for Pr = 20,000.

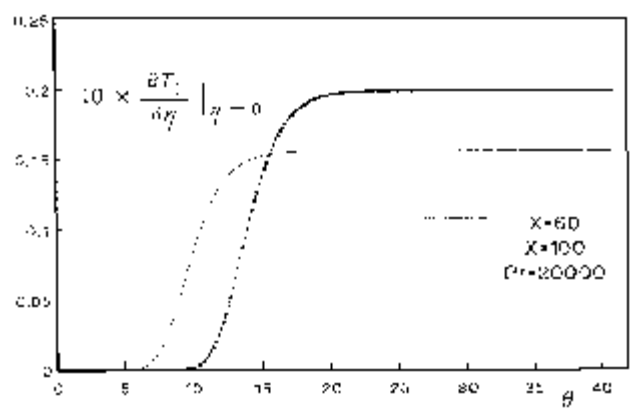

Figure 12. Gradient of T_1 on the wall at X = 100 (---) and X = 60 (- - -) for Pr = 20,000.

second-order outer velocity at Pr= 50000 for different values of q. Figure 9 shows the variation of velocity obtained from complete numerical solution of the equations (---) and the perturbation solution (- - -) at Pr= 16 for different values of t and as it is seen these two curves compare very well, except near the maximum values of the velocity. The error in complete solution of the equations increases by increase of Prandtl number. Figure 10 shows the variation of velocity for Pr= 20 (---) and Pr= 1000 (- - -) for different values of q using perturbation methods. By increase of Pr the maximum values of velocity gets closer to the wall and the thickness of the thermal boundary layer decreases. Figures 11-13 show the gradients of T_0, T_1, and T_2 on the wall, respectively. Comparing each figure at X = 60 and X = 100 is interesting. Figure 14 shows

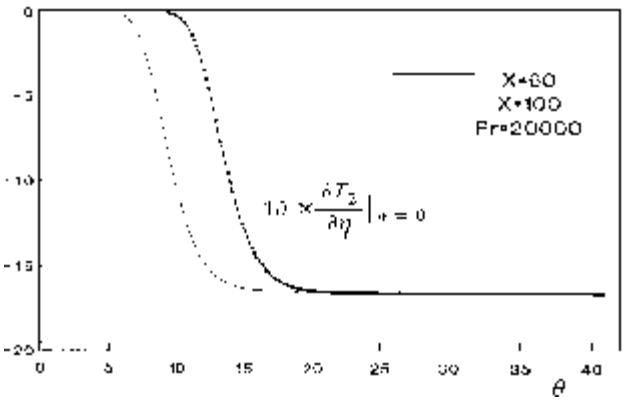

Figure 13. Gradient of T_2 on the wall at X = 100 (---) and X = 60 (- - -) for Pr = 20,000.

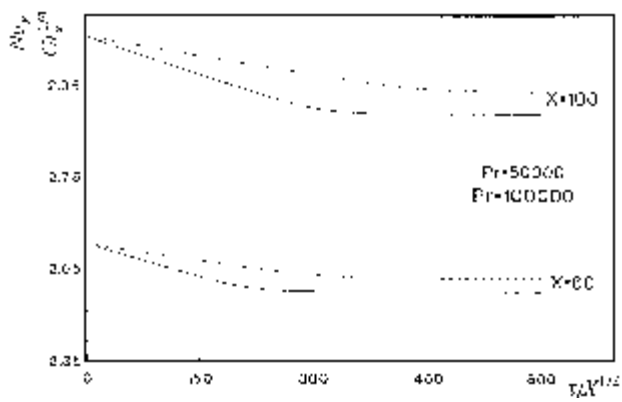

Figure 14. $Nu_x / Gr_x^{1/4}$ versus $\tau / X^{1/2}$ at X = 100 and X = 60 for Pr = 50,000 (---) and Pr = 100,000 (- - -).

$Nu_x / Gr_x^{1/4}$ versus $\tau / X^{1/2}$ at Pr=50000 (---) and Pr = 100000 (- - -) for X = 60 and X = 100. It is seen that local Nusselt number is greater for bigger X and this is the same as the Ostrach [9] results.

CONCLUSIONS

The results of the present study indicate that, at high Prandtl number, the transient natural convection flow near a vertical isothermal surface is also characterized by two layers. Here the velocity boundary layer tends to be somewhat larger due to large kinematic viscosity relative to thermal diffusivity. The motion of the outer layer, however, seems to be caused by the drag force exerted by the inner layer, not due to the buoyancy itself. This dual-layer structure is characteristic of the transient flow which results from a step change in the temperature of a vertical isothermal surface. Using the method of matched asymptotic expansions, and matching at each time step and x location, it is possible to numerically calculate time-dependent expansion solutions for the inner and outer regions. These may be combined to form uniformly-valid time-dependent solutions for any large Prandtl number. The three-term composite expansions were found to be in good agreement with the numerically calculated solution of the full equations for Prandtl number at least as low as 16.

As Pr $\to \infty$, the overshoot in the local Nusselt number disappears. This suggests that at large Pr, the Nusselt number may be calculated with fair accuracy during the transient by using the value predicted by the one-dimensional closed-form solution until its value equals the steady-state value. After that point, the steady-state value would be used.

In the modified form used here, the method of matched asymptotic expansions proved to be an effective techniques for analysis of the transient natural convection flow resulting from a step change in surface temperature.

NOMENCLATURE

A_{KJ} B_{KJ}	functions determined by matching
Gr_x	Grashof number
g	acceleration of gravity
h_x	local heat transfer coefficient
Nu_x	Nusselt number
Pr	Prandtl number
t	time
T	dimensionless temperature
T_i	inner region temperature
T_w	wall temperature
T_∞	fluid temperature
U, V	dimensionless velocity
U_i, V_i	inner region velocity
U^o, V^o	outer region velocity

u, v	components of velocity Parallel and normal to the surface
X, Y	dimensionless coordinates
x, y	vertical and horizontal coordinates

GREEK

e	Perturbation Parameter
b	Coefficient of thermal expansion
h	inner stretched Coordinate
q	stretched time variable
n	Kinematic viscosity
x	outer stretched coordinate
t	dimensionless time

APPENDIX

ε^0 :

$$\frac{\partial U_0}{\partial X} + \frac{\partial V_0}{\partial \eta} = 0$$

$$\frac{\partial^2 U_0}{\partial \eta^2} + T_0 = 0$$

$$\frac{\partial T_0}{\partial \theta} + U_0 \frac{\partial T_0}{\partial X} + V_0 \frac{\partial T_0}{\partial \eta} = \frac{\partial^2 T_0}{\partial \eta^2} \qquad \text{(I)}$$

$\varepsilon^{1/2}$:

$$\frac{\partial U_1}{\partial X} + \frac{\partial V_1}{\partial \eta} = 0$$

$$\frac{\partial^2 U_1}{\partial \eta^2} + T_1 = 0$$

$$U_1 \frac{\partial T_0}{\partial X} + V_0 \frac{\partial T_1}{\partial \eta} +$$

$$+ V_1 \frac{\partial T_0}{\partial \eta} - \frac{\partial^2 T_1}{\partial \eta^2} \qquad \text{(II)}$$

ε^1 :

$$\frac{\partial U_2}{\partial X} + \frac{\partial V_2}{\partial \eta} = 0$$

$$\frac{\partial^2 U_2}{\partial \eta^2} + T_2 = 0$$

$$\frac{\partial T_2}{\partial \theta} + U_0 \frac{\partial T_2}{\partial X} + U_1 \frac{\partial T_1}{\partial X} + U_2 \frac{\partial T_0}{\partial X}$$

$$V_0 \frac{\partial T_2}{\partial \eta} + V_1 \frac{\partial T_1}{\partial \eta} + V_2 \frac{\partial T_0}{\partial \eta} = \frac{\partial^2 T_2}{\partial \eta^2} \qquad \text{(III)}$$

ε^0 :

$$\frac{\partial u_0}{\partial X} + \frac{\partial v_0}{\partial \xi} = 0$$

$$\frac{\partial u_0}{\partial \theta} + u_0 \frac{\partial u_0}{\partial X} + v_0 \frac{\partial u_0}{\partial \xi} = \frac{\partial^2 u_0}{\partial \xi^2} \qquad \text{(IV)}$$

$\varepsilon^{1/2}$:

$$\frac{\partial u_1}{\partial X} + \frac{\partial u_1}{\partial \xi} = 0$$

$$+ u_1 \frac{\partial u_0}{\partial X} + v_0 \frac{\partial u_1}{\partial \xi} +$$

$$v_1 \frac{\partial u_0}{\partial \xi} - \frac{\partial^2 u_1}{\partial \xi^2} \qquad \text{(V)}$$

ε^1 :

$$\frac{\partial u_2}{\partial X} + \frac{\partial v_2}{\partial \xi} = 0$$

$$v_0 \frac{\partial u_2}{\partial \xi} + v_1 \frac{\partial u_1}{\partial \xi} + v_2 \frac{\partial u_0}{\partial \xi} - \frac{\partial^2 u_2}{\partial \xi^2} \qquad \text{(VI)}$$

$$A_{10}(X,\theta) = \lim_{\eta \to \infty} U_0(X,\theta,\eta)$$

$$A_{11}(X,\theta) = \lim_{\eta \to \infty} \left[U_1(X,\theta,\eta) \right.$$

$$\left. A_{\perp}(X,\theta) \cdot \eta \right]$$

$$A_{11}(X,\theta) = \frac{\partial u_0}{\partial \xi}(X,0,\theta)$$

$$\theta,\eta)$$

$$A_{21}(X,\theta)\cdot\eta \quad A_{22}(X,\theta)\cdot\frac{\eta^2}{2}\Big]$$

$$A_{21}(X,\theta) = \frac{\partial u}{\partial \xi}(X,0,\theta)$$

$$\text{(VII)}\quad A_{22}(X,\theta) = \frac{\partial^2 u_0}{\partial \xi^2}(X,0,\theta)$$

REFERENCES

1. Siegel, R., "Transient Free Convection from a Vertical Flat Plate", ***Trans. Am. Soc. Mech. Engrs.***, 80, (1958), 347-359.
2. Midelman, S., "An Introduction to Mass and Heat Transfer", John Wiley and Sons, (1998).
3. Bejan, A., "Convection Heat Transfer", John Wiley and Sons, New York, (1995).
4. Pop, I., Yan, B., Ingham, D. B., "Free Convection from a Horizontal Moving Sheet", ***Heat and Mass Transfer***, 31, Springer, (1995), 57-64.
5. Gebhart, B., "Transient Natural Convection from Vertical Elements", ***Trans. Am. Soc. Mech. Engrs.***, Series C, ***J. Heat Transfer***, 83, (1961), 61-70.
6. Kevorkian, J. and Cole, J. D., "Multiple Scale and Singular Perturbation Method", Springer (1996).
7. Hellums, J. D. and Churchill, S.W., "Transient and Steady State Free and Natural Convection, Numerical Solutions: Part I. The Isothermal, Vertical Plate", ***A. L. Ch. E. J.***, L8, (1991), 690-692.
8. Nayefeh, A. H., "Introduction to Perturbation Techniques", John Wiley and Sons, New York, (1993).
9. Ostrach, S., "An Analysis of Laminar Free-Convection Flow and Heat Transfer About a Flat Plate Parallel to The Direction of The Generating Body Force", NACA TN 2636 (1952).